Springer

Journal of Mechanical Science and Technology 22 (2008) 1602~1611

Journal of Mechanical Science and Technology

www.springerlink.com/content/1738-494x
DOI 10.1007/s12206-008-0417-6

Study on operating characteristics of fuel cell powered electric vehicle with different air feeding systems

Junghwan Bang[1], Han-Sang Kim[2], Dong-Hun Lee[3] and Kyoungdoug Min[2,*]

[1]*School of Mechanical and Aerospace Engineering/SNU-IAMD, Seoul National University, 599 Gwanangno, Gwanak-gu, Seoul, 151-742, Korea*

[2]*School of Mechanical and Aerospace Engineering, Seoul National University, 599 Gwanangno, Gwanak-gu, Seoul, 151-742, Korea*

[3]*R&D Centre, Hyundai-Kia Motor Company, Mabook-dong, Giheung-gu, Yongin-si, Gyunggi-do, 446-716, Korea*

(Manuscript Received December 20, 2007; Revised March 3, 2008; Accepted April 19, 2008)

Abstract

In this paper the modeling of a fuel cell powered electric vehicle is presented. The fuel cell system consisting of a proton exchange membrane (PEM) fuel cell stack and balance of plant (BOP) was co-simulated with a commercial vehicle simulation program. The simulation program calculates the load of the fuel cell depending on the driving mode of the vehicle and also calculates the overall efficiency and each parasitic loss by applying the load in the fuel cell model that is used to estimate the performance of the entire vehicle system by calculating the acceleration performances and fuel economy of the vehicle. Two types of air feeding systems (blower type and compressor type) were modeled by using MATLAB/Simulink environment and the effect of fuel cell stack size (number of cells, cell area) on the fuel economy and performance of the fuel cell powered vehicle was investigated. Using a driving cycle of FTP-75, the required power, BOP component power loss, and system efficiency for two types of fuel cell systems were analyzed. Through this study, we could get a basic insight into the fuel cell powered electric vehicle and its characteristics.

Keywords: Fuel cell powered vehicle; Simulation; PEM; BOP; Fuel economy; System efficiency

1. Introduction

To reduce air pollution due to exhaust emissions from vehicles, the fuel cell is recognized as a promising alternative power source for next-generation vehicles [1, 2]. The proton exchange membrane (PEM) fuel cell is considered to be an attractive power source for automotive application because of its high efficiency, low-operating temperature, high power density, and modular design [3, 4]. Therefore, for the past several years, the world automobile manufacturers have been performing active research work on PEM fuel cell powered vehicles. Recent research and development of fuel cell technology for automotive applications are focused on system based research and optimization work on the fuel cell system with auxiliary components (altogether named as balance of plant (BOP)) to improve the efficiency and performance of the whole vehicle system [5]. The key parameters which determine the efficiency and performance of the fuel cell system are the cell temperature, supplied air pressure, and supplied gas humidity. Overall stack efficiency generally depends on the output current of the fuel cell. Therefore, if the number of stacked cells is increased for equal power requirement, higher efficiency can be obtained. However, the increase in mass of the fuel cell system has a negative effect on the efficiency and performance of a vehicle. Hence, there exists some trade-off between efficiency of the fuel cell system and vehicle weight.

Since the first invention of the fuel cell, many researchers have investigated the fuel cell vehicle system and its efficiency [6, 7]. Wipke et al. carried out

*Corresponding author. Tel.: +82 2 880 1661, Fax.: +82 2 883 0179
E-mail address: kdmin@snu.ac.kr

the modeling of the vehicle simulation program named ADVISOR (ADvanced VehIcle SimultOR) [8, 9] and estimated the fuel economies and acceleration performances of various kinds of power-trains. The included fuel cell model was a very simple model that comes from experimental data of the ANL (Argonne National Laboratory) and this model has simple look-up tables such as a table of the required power and hydrogen usage amount only. Friedman et al. [10] analyzed the efficiency and cost of the fuel cell vehicle through the research of the hybridization of a fuel cell vehicle. Cunningham et al. [11] and Doss et al. [12] investigated the differences between two types of air feeding systems (low-pressure and high-pressure) and the modelings of air feeding systems were performed. Sadler et al. [13] suggested the method of modeling techniques of fuel cell vehicle applications. Jeong and Oh [14] and Hussain et al. [15] applied fuel economy and life-cycle cost analysis to the fuel cell hybrid vehicle. However, the above researches cannot explain how the parasitic losses of BOP components are characterized. Therefore, the ANL tested the Honeywell compressor-expander-module and applied it to the fuel cell system and vehicle simulation. Liang and Qingnian [16] compared the performance of fuel cell sedan with ICE (Internal Combustion Engine) sedan using vehicle simulation. Ahluwalia [17], Maxoulis [18], and Hou [19] modeled the fuel cell vehicle system from the empirical equations and obtained the fuel economy of the fuel cell vehicles. Kim and Peng [20] modeled fuel cell hybrid vehicle and optimized its operating parameters. In this paper the power distribution of the fuel cell vehicle was analyzed and the system management of the fuel cell system and air pressure was investigated.

For a fuel cell system, two types of air feeding systems exist; the blower-type and the compressor-type. It becomes possible to determine the loss distribution, as well as the advantages and disadvantages related to these two types of fuel cell systems by performing simulation after applying the models of two types of fuel cell systems [17, 21]. The fuel cell system with the blower-type of air feeding system has a simple structure, thereby enabling easier control. However, its main disadvantage is that it is not possible to obtain the maximum performance as a fuel cell. On the other hand, in case of the fuel cell system with the compressor-type air feeding system, the control is not easy; however, it is possible to obtain the maximum performance, thereby reducing the number of fuel cells. Studies on air feeding systems have been carried out continuously. And in this study, the overall fuel economy and loss within BOP depending on the air feeding system in a fuel cell powered vehicle will be presented.

The objectives of this work are the modeling of the blower type and compressor type fuel cell and the investigation of the effect of system mass and other parameters on fuel economy and performance of the fuel cell powered electric vehicle. And the main operating points of two types of fuel cell systems are presented.

2. Modeling of fuel cell system

In this study two different fuel cell operating systems were used according to air feeding pressure. Fig. 1 shows the lower-pressure operating system using a blower for air feeding. The higher-pressure system using a compressor for supplying air to the cathode side is indicated in Fig. 2. For the ease of model generation and connected simulation, all the codes were made in MATLAB/Simulink environment, and these were then simulated along with the vehicle simulation program.

2.1 Fuel cell stack

The fuel cell model was based on the mechanistic models [22, 23]. It contains the open circuit

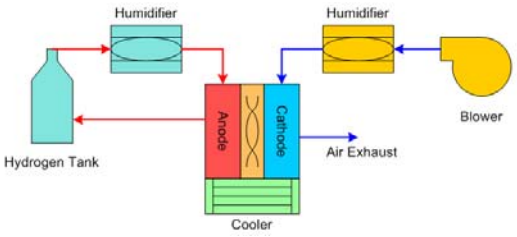

Fig. 1. Schematic diagram of blower type fuel cell system.

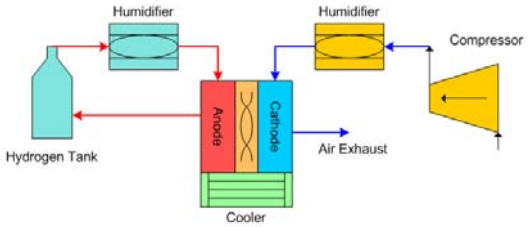

Fig. 2. Schematic diagram of compressor type fuel cell system.

voltage, activation loss, ohmic loss, and concentration loss models. This model can be affected by some important operating parameters of the fuel cell stack such as hydrogen pressure, air pressure, cell average temperature, cell number, cell area, and so on. In this study, the cell area is fixed to 400 cm^2 (20 cm × 20 cm) and the number of stacked cells can be changed for fuel cell stack sizing. Air and hydrogen stoichiometric ratios are maintained to 2 and 1.2. Voltage of each unit cell is calculated by Eqs. (1)-(4)

$$V_{fc} = E - V_{act} - V_{ohm} - V_{conc} \tag{1}$$

where E is open circuit voltage, V_{act} is the activation loss, V_{ohm} is the ohmic loss and V_{conc} is the concentration loss. Eqs. (2)-(4) calculate the activation loss, the ohmic loss, and the concentration loss.

$$V_{act} = a \ln\left(\frac{i}{i_o}\right) v_0 + v_a(1 - e^{-c_1 i}) \tag{2}$$

$$V_{ohm} = i R_{ohm} \tag{3}$$

$$V_{conc} = i\left(c_2 \frac{i}{i_l}\right)^{c_3} \tag{4}$$

The open circuit voltage is calculated from the chemical energy balance [24].

$$E = 1.229 - 0.85\times10^{-3}(T_{fc} - 298.15) + 4.3085\times10^{-5} T_{fc}\left[\ln(p_{H_2}) + \frac{1}{2}\ln(p_{O_2})\right] \tag{5}$$

where T_{fc} is cell temperature and p is partial pressure of each species. From previous studies [25], the ohmic resistance of membrane can be a function of the membrane thickness (t_m) and the membrane conductivity (σ_m).

$$R_{ohm} = \frac{t_m}{\sigma_m} \tag{6}$$

The membrane conductivity is a function of membrane humidity and fuel cell temperature.

$$\sigma_m = b_1 \exp\left(b_2\left(\frac{1}{303} - \frac{1}{T_{fc}}\right)\right) \tag{7}$$

where b_1 and b_2 are constants. In this study, the empirical values from [25] are used.

In order to obtain v_0 and other constants, Pukrushpan [22] fitted equations to the empirical results. The regression equations are

$$v_0 = 0.279 - 8.5\times10^{-4}(T_{fc} - 298.15) + 4.308\times10^{-5} T_{fc}\left[\ln\left(\frac{p_{ca} - p_{sat}}{1.01325}\right)\right] + \frac{1}{2}\ln\left(\frac{0.1173(p_{ca} - p_{sat})}{1.01325}\right)$$

$$v_a = (-1.618\times10^{-5} T_{fc} - 1.618\times10^{-2})\left(\frac{P_{O_2}}{0.1173} + P_{sat}\right)^2 + (1.8\times10^{-4} T_{fc} - 0.166)\left(\frac{P_{O_2}}{0.1173} + P_{sat}\right) + (-5.8\times10^{-4} T_{fc} + 0.5736)$$

$$c_2 = \begin{cases} (7.16\times10^{-4} T_{fc} - 0.622)\left(\frac{P_{O_2}}{0.1173} + P_{sat}\right) + (-1.45\times10^{-3} T_{fc} + 1.68) \\ \quad \text{for } \left(\frac{P_{O_2}}{0.1173} + P_{sat}\right) < 2\,atm \\ (8.66\times10^{-5} T_{fc} - 0.068)\left(\frac{P_{O_2}}{0.1173} + P_{sat}\right) + (-1.6\times10^{-4} T_{fc} + 0.54) \\ \quad \text{for } \left(\frac{P_{O_2}}{0.1173} + P_{sat}\right) \geq 2\,atm \end{cases}$$

$$c_1 = 10, \quad i_1 = 2.2, \quad c_3 = 2 \tag{8}$$

It is assumed that the same unit cells are used in two types of fuel cell systems. However, the numbers of stacked cells are different. The maximum power of fuel cell systems are calculated values from the each model and parasitic losses are considered.

2.2 Humidifier

The humidifier system consists of the membrane type and the bubbling type. Humidity of reacting gases must be supplied to allow the proton exchange membrane to transfer protons easily and to control water flooding in the cathode electrode. The membrane type humidifier can humidify air and hydrogen to about 56%. Water is partially supplied from the condensed water in the exhaust gas of a fuel cell system. Insufficient humidity was supplied by the bubbling type humidifier. The bubbling type humidifier was used to supply water vapor to the hydrogen and air of the fuel cell. In this work the electrical power from the fuel cell stack is supplied to the electrical heater for evaporation of water and for the feeding pump. Efficiencies in the pump and heater were assumed to be constant [26, 27].

For the first cases, the humidifier system that has the membrane and bubbling type was used for calculating fuel economy and the power distribution is

shown in Table 2. And for the second case, the humidifier system that has the membrane type only was used for calculating power distribution of parasitic losses in Table 3.

2.3 Air feeding system

Two different types of air supplying systems (blower type and compressor type) were applied. The blower type system gives constant inlet air pressure of the fuel cell stack and air inlet pressure can be controlled for the compressor type system [17]. Efficiency and power of these systems were calculated by the performance chart in the look-up-table form. Air mass flow rate is calculated by Eq. (9).

$$\dot{m}_{air} = 3.57 \times 10^{-7} \times \lambda_{air} \times \frac{w_s}{v_{fc}} \tag{9}$$

For more power density, other types of fuel cell systems use compressors as their air feeding systems. If the inlet air pressure is increased, the chemical reaction is more active. Therefore, we can get more power compared to a blower type fuel cell system. However, the power requirement of the compressor type system is larger than that of the blower type system. In this paper during vehicle driving mode, power loss distributions in each fuel cell system were compared with each other. Power consumed in the compressor is calculated by Eq. (10).

$$\text{Power} = C_p \frac{T_1}{\eta_c \eta_m} \left[\left(\frac{P_2}{P_1} \right)^{\frac{\gamma-1}{\gamma}} - 1 \right] \dot{m}_{air} \tag{10}$$

2.4 Stack cooler

To prevent excessive temperature rise of the fuel cell stack, water is used as a coolant. Cooling water tubes are located in bipolar plates and water is supplied out of the system to each selected bipolar plate. It is assumed that all the heat from the fuel cell stack is transferred to the cooling water. One cooling water plate is located between two fuel cell plates and it is assumed that there are 100 tubes in one cooling water plate. The inlet and outlet pressure of the cooling water and mass flow rate were calculated and the required pump power can be calculated using Eqs. (11)-(13).

$$W_S \left(\frac{E}{v_{fc}} - 1 \right) = \dot{m}_{cw} C_p \Delta T_{cw} = hA(T_{fc} - T_{cw}) \tag{11}$$

$$\Delta p_{drop} = H \rho_{cw} g \tag{12}$$

$$\text{pump power} = \frac{\Delta p_{drop} \dot{m}_{cw}}{\eta_v \eta_m \eta_h \rho_{cw}} \tag{13}$$

3. Fuel cell vehicle modeling

The fuel cell powered vehicle model is shown in Fig. 3. Fuel cell powered vehicle simulation is classified into two parts. The vehicle part was simulated by a vehicle simulation program developed at Seoul National University and it calculates the driving cycle data of vehicle and transmission and the required power of the motor. The fuel cell system part was simulated by MATLAB/Simulink environment and it can calculate the fuel cell system power, efficiency, and auxiliary electrical load. The detailed vehicle specifications used for this study are summarized in Table 1.

An electric permanent magnet motor model of 49 kW in ADVISOR was adopted for vehicle simulation. This motor capacity is acceptable for a small vehicle considering its acceleration performance and maximum velocity. According to its speed and torque, the efficiency of the motor was calculated and in MATLAB, the required power of the motor was calculated using look-up-table. Fig. 4 shows 49 kW motor maximum torque. From driver module the required torque is calculated and torque is applied to the transmission. Its efficiency is shown in Fig. 5.

Table 1. Vehicle model specification.

Description	Specification
Vehicle mass w/o fuel cell system (kg)	838
Coefficient of aerodynamic drag	0.335
Frontal area (m^2)	2.0
Final gear ratio	5.67
Motor power (kW)	49

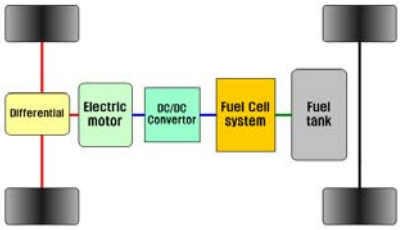

Fig. 3. Schematic diagram of fuel cell powered vehicle.

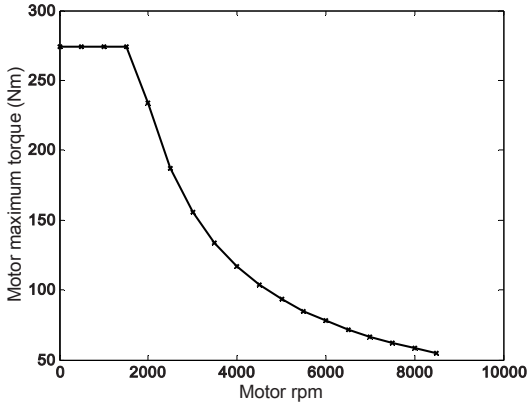

Fig. 4. Maximum torque characteristics of the electric motor.

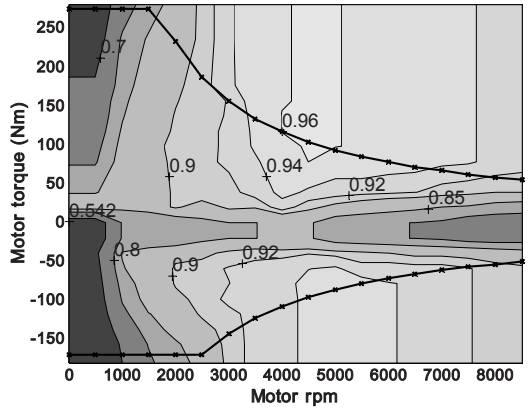

Fig. 5. Motor efficiency.

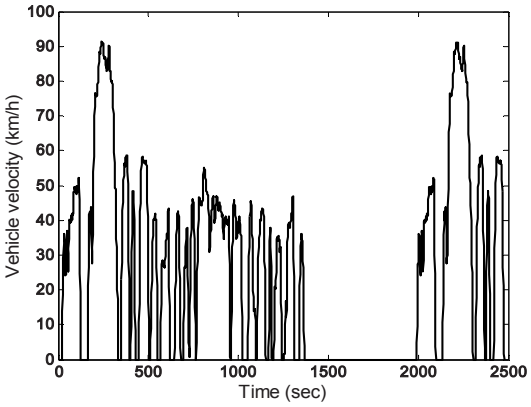

Fig. 6. Velocity profile of drive cycle FTP-75.

DC/DC converter is a transformer that can receive the electric power from the fuel cell system and transfer the proper voltage and current to an electric motor. Its efficiency is assumed to be constant at 90% [28]. Electrical accessory load was fixed to 700 W.

A vehicle equipped with a conventional engine needs a complex transmission such as MT, AT, or CVT to have guaranteed torque characteristics in low engine speed. However, an electric motor does not need a complex transmission because of its high torque in low motor speed. Therefore, in this model, final gear ratio (FGR) is selected only and it simplifies the model. Its efficiency is fixed at 97%.

In this study FTP-75 mode is selected as a driving cycle as indicated in Fig. 6. This driving cycle is typically used for fuel economy and exhaust emission testing of passenger vehicles [29].

It is important as to how we can describe a real driver's behavior in simulation code. The input signal of the driver model is the desired vehicle speed and the output signal consists only of the acceleration and brake pedal signal. However, if its control is not compatible to this vehicle model, it cannot be operated in the desired speed range. Therefore we determined control gains by trial-and-error method and in this study the speed error is lower than 3%.

From the fuel cell model we can get optimal parameters like air, hydrogen humidity, air pressure, etc. Especially in the compressor type model, the operating pressure is the most important key parameter because this parameter affects the fuel cell power and parasitic loss (compressor loss) largely. Therefore varying these parameters the variation of the fuel cell system efficiency is observed and the highest efficiency points can be obtained. In this paper the operating pressure is determined by choosing the point that the system efficiency is the highest among the required power and temperature condition and optimal pressure values are applied to the fuel cell vehicle simulation.

4. Simulation results

4.1 Variation of fuel cell system power

The maximum power of a fuel cell system is mainly affected by the number of cells, cell area, unit cell characteristic, and power loss of BOP. The fuel economy and efficiency of the fuel cell system according to the maximum power for the blower type are shown in Fig. 7. The efficiency of the fuel cell system is the average value throughout the drive cycle. The efficiency of the fuel cell system increases when the maximum power of the fuel cell system is increased. This is because the fuel cell system operates

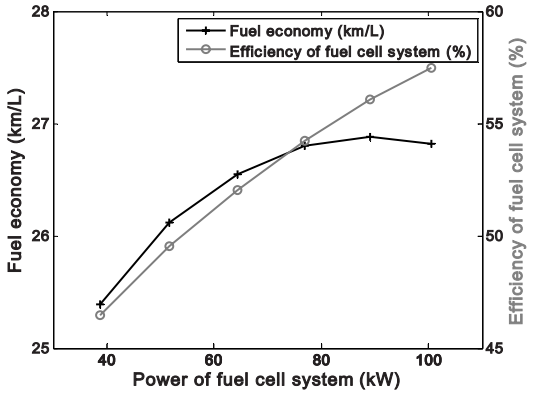

Fig. 7. Fuel economy and system efficiency trends of blower type system.

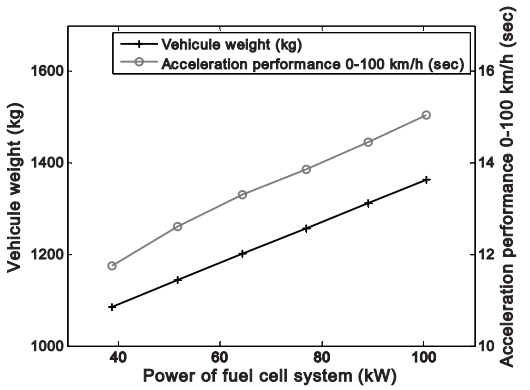

Fig. 8. Vehicle weight and acceleration performance of blower type system.

in a lower current range where the fuel cell efficiency is higher. When the maximum power of the fuel cell system exceeds 89 kW, the fuel economy depends more on vehicular weight than on the efficiency of the fuel cell system. Fuel cell system, which has 700 unit cells, can produce 89kW as the maximum power. The fuel economy is maximized at the power of 89 kW due to trade-off between the vehicle weight and the efficiency of the fuel cell system.

Fig. 8 shows the vehicular weight and acceleration performance as a function of maximum power for the blower type fuel cell system. Vehicular weight is the most important parameter for the vehicle acceleration performance. The acceleration performance for the maximum fuel cell system power depends largely on the vehicular weight and it is irrespective of maximum power of the fuel cell system. This is due to the fact that the maximum power of the electric motor is fixed to 49 kW.

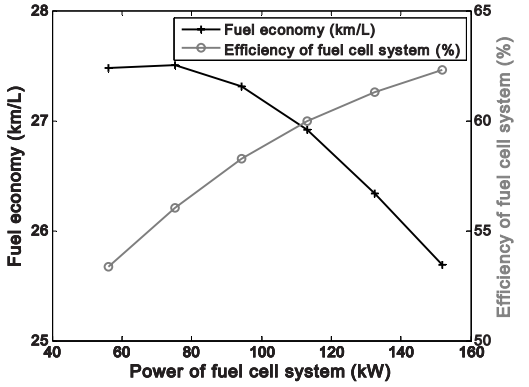

Fig. 9. Fuel economy and system efficiency trends of compressor type system.

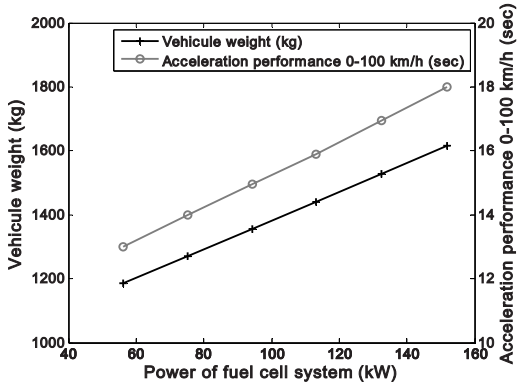

Fig. 10. Vehicle weight and acceleration performance of compressor type system.

Fig. 9 indicates the fuel economy and efficiency of the fuel cell system according to the maximum power of the compressor type system. The maximum point of fuel economy is located at the power of 75 kW. In the case of the compressor type the inlet air is pressurized. Therefore, electrochemical reaction can be done easily, so power density of the compressor type is larger than that of the blower type. The x-axes of Fig. 7 and Fig. 9 are the power of the fuel cell system that the same number of plates was stacked.

Fig. 10 shows the vehicular weight and acceleration performance according to maximum power for the compressor type. To obtain a higher efficiency, inlet air pressure is optimized to the points where the efficiency of the fuel cell system is best [30]. An optimized pressure map is presented in Fig. 11. For the compressor type fuel cell system, the effect of vehicular weight on fuel economy is larger than that of the blower type system because in the same level of power, the weight of the compressor type is two

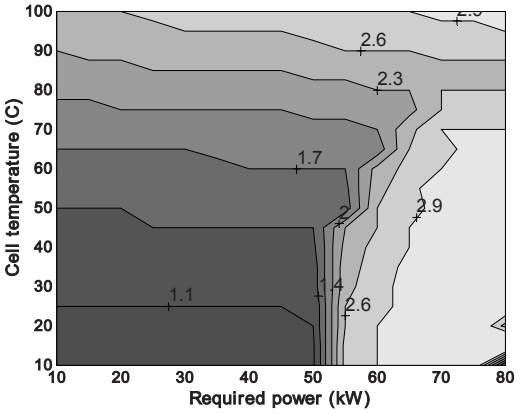

Fig. 11. Optimized air pressure (bar).

thirds lighter than that of the blower type. Therefore, there is a maximum point of fuel economy in a smaller maximum power system although it shows higher efficiency. Furthermore, it is found that the efficiency of the fuel cell system at high maximum power (120~140 kW) is converged to constant value. The weight of the fuel cell stack and BOP are generally proportional to the maximum power .

4.2 Comparison of blower and compressor type systems

In case of the fuel cell system, cathode air pressure is a very important parameter for enhancing system efficiency. If the air is pressurized, the partial pressure of oxygen in the fuel cell is increased and ideal voltage loss can be reduced as represented in Eq. (14). Therefore, the compressor type fuel cell system can be more compact than the blower type. However, the weight of BOP components for the compressor type becomes heavier than that for the blower type.

$$E = E_0 - \frac{RT}{2F} ln \frac{1}{p_{H_2} p_{O_2}^{1/2}} \quad (14)$$

Table 2 shows simulated results during the driving cycle for two types of fuel cell systems with the same maximum net power level. The mass of the fuel cell system of the compressor type is 20 kg heavier than that of the blower type if they have the same amount of fuel cell stack power. The blower type has a stack with smaller stacked cells. Therefore, the mass of the compressor type vehicle is about 65 kg lighter than that of the blower type. For stack work, the blower type produces more work because of its lower efficiency of fuel cell system. Since the weight of the blower type fuel cell system is heavier and its thermal capacity is higher than that of the compressor type, the cooling pump work for the blower type is a little smaller than that of the compressor type. Required work for the humidifier of the blower type is larger than that of the compressor type. That is due to the fact that less heat is needed to vaporize the water because of the temperature rise in compressed air exiting the compressor. Fig. 12 indicates cycle operating points and efficiency contours for two types of fuel cell systems. The compressor type system operates in relatively higher current ranges; however, its efficiency in a lower current range is higher than that of the blower type [31]. Therefore, the overall driving cycle efficiency of the compressor type becomes higher than that of the blower type. Fig. 13 shows the air feeding work of two types of fuel cell systems in the vehicle driving mode. If the required power is increased and cell temperature is increased as time goes by, in blower type an additional work is not needed except for high load regions, while in compressor type required work for air feeding is increased continuously. However, in the blower type more humidifier work is needed as indicated in Fig. 14, because the heat from the compression process helps with water evaporation. Calculated parasitic losses of two fuel cell systems are shown in Fig. 15. When time is up to 2,000 seconds, the blower type system needs more work for the humidifier to evaporate the

Table 2. Detailed comparisons of blower and compressor type systems with the membrane and bubbling type humidifier in typical drive cycle (FTP-75).

Description	Blower type	Compressor type
Maximum fuel cell system power (kW)	76.9	74.7
hydrogen mass * LHV (kJ)	21399.0	19574.3
Fuel cell system work (kJ)	10584.3	9926.2
Stack work (kJ)	14102.6	12248.8
Cooling pump work (kJ)	1.0	1.4
Air feeding work (kJ)	1786.0	2428.63
Humidifier work (kJ)	1903.4	253.7
Fuel cell system efficiency (%)	46.3	50.7
Electric motor efficiency (%)	85.8	85.8
Overall drive cycle efficiency (%)	27.7	28.5

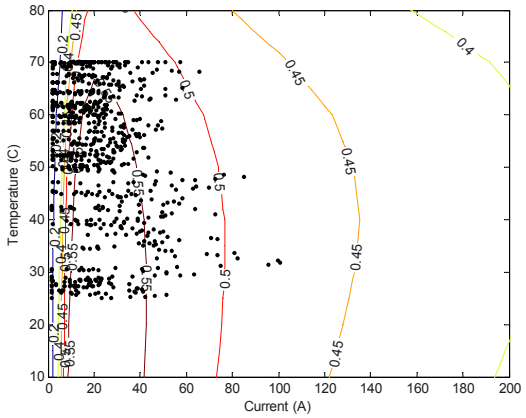

(a) Blower type

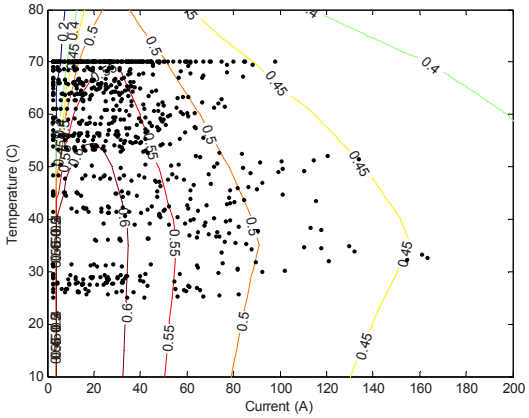

(b) Compressor type

Fig. 12. Cycle operating points and efficiency contours of two types of fuel cell systems.

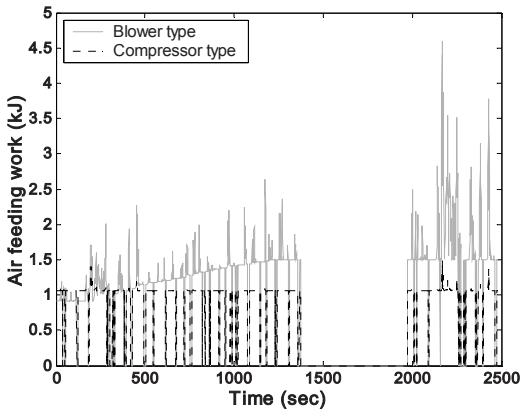

Fig. 13. Comparison of air feeding loss work (Blower type and compressor type).

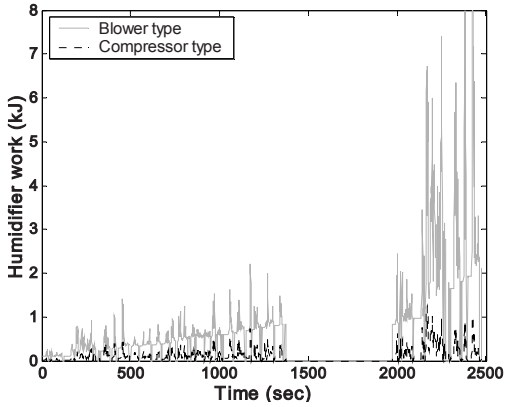

Fig. 14. Comparison of humidifier power loss work (Blower type and compressor type).

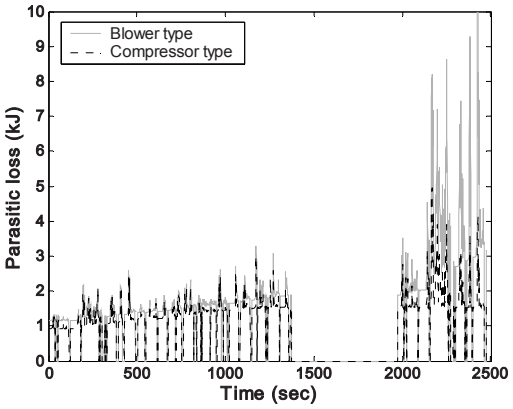

Fig. 15. Comparison of parasitic loss (Blower type and compressor type).

water.

Detailed power distribution of a fuel cell vehicle with membrane type humidifier only is shown in Table 3. The stack work of the fuel cell system with compressor is larger than that of the fuel cell system with blower, because these systems use the membrane type humidifier only and the parasitic loss of the humidifier is zero. Therefore the humidifier of the bubbling type is not good for the fuel cell vehicle application and the membrane performance of the humidifier can determine the entire efficiency of the fuel cell system. In addition, research on the membrane has to be done for low fuel consumption of the fuel cell powered vehicle.

Fig. 16 shows fuel economy results in different driving modes. In general, the compressor type system indicates slightly higher fuel economy; however it is almost the same. If the more efficient compressor

Table 3. Detailed comparisons of blower and compressor type systems with the membrane type humidifier only in typical drive cycle (FTP-75).

Description	Blower type	Compressor type
Maximum fuel cell system power (kW)	74.4	74.7
hydrogen mass * LHV (kJ)	20401.6	22927.7
Fuel cell system work (kJ)	10780.2	10894.7
Stack work (kJ)	12503.1	13681.9
Cooling pump work (kJ)	1.8	3.3
Air feeding work (kJ)	1700.4	3127.3
Humidifier work (kJ)	0	0
Fuel cell system efficiency (%)	53.8	47.5
Electric motor efficiency (%)	85.8	85.8
Overall drive cycle efficiency (%)	32.6	29.4

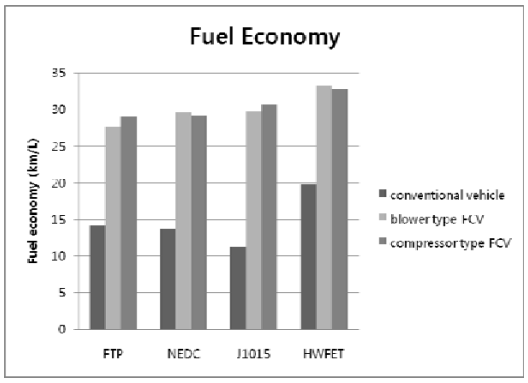

Fig. 16. Comparison of fuel economy in various drive cycle.

is used, the compressor type system can show higher fuel economy.

5. Conclusions

The modeling of two types of fuel cell systems (blower type and compressor type) and the fuel cell powered electric vehicle were performed. Through the simulation of a typical drive cycle (FTP-75), two types of fuel cell systems are compared in the views of fuel economy and performance. The major findings from this study can be summarized as follows;

(1) There is an optimal point in power variation of the fuel cell system in fuel economy and that is due to the combined effect of vehicular mass and the efficiency of the fuel cell system.

(2) The main power loss of the fuel cell system of the blower type is the power for driving the humidifier module. As well, the main power loss of the fuel cell system of the compressor type is for the electrically driven compressor. The required load for the cooling module is relatively small compared to power losses for other BOP components.

(3) The efficiency of the fuel cell system of compressor type is about 4.8% higher than that of the blower type in FTP-75 mode. The compressor type produces better fuel economy for overall driving than the blower type.

(4) Through this study we can get a basic insight into fuel economy and power distribution between system components in a vehicle that is solely powered by fuel cell.

Acknowledgements

This research was supported (in part) by SNU-IAMD.

References

[1] M. Ahman, Primary energy efficiency of alternative powertrains in vehicles, Energy, 26 (11) (2001) 973-989.

[2] A. Schafer, J. B. Heywood, and M. A. Weiss, Future fuel cell and internal combustion engine automobile technologies: A 25-year life cycle and fleet impact assessment, Energy, 31 (12) (2006) 2064-2087.

[3] S. Srinivasan, O. A. Velev, A. Parthasarathy, D. J. Manko, and A. J. Appleby, High energy efficiency and high power density proton exchange membrane fuel cells -- electrode kinetics and mass transport, Journal of Power Sources, 36 (3) (1991) 299-320.

[4] P. Corbo, F. Migliardini, and O. Veneri, Performance investigation of 2.4 kW PEM fuel cell stack in vehicles, International Journal of Hydrogen Energy, 32 (17) (2007) 4340-4349.

[5] N. Johnson, Development of a PEM Fuel Cell Simulation Model for Use in Balance of Plant Design, SAE, 2004-01-1468 (2004).

[6] K. Haraldsson and K. Wipke, Evaluating PEM fuel cell system models, Journal of Power Sources, 126 (1-2) (2004) 88-97.

[7] B. Sorensen, On the road performance simulation of

hydrogen and hybrid cars, International Journal of Hydrogen Energy, 32 (6) (2007) 683-686.

[8] M. J. Ogburn, D. J. Nelson, K. Wipke, and T. Markel, Modeling and Validation of a Fuel Cell Hybrid Vehicle, SAE, 2000-01-1566 (2000).

[9] T. Markel, A. Brooker, T. Hendricks, V. Johnson, K. Kelly, B. Kramer, M. O'Keefe, S. Sprik, and K. Wipke, ADVISOR: a systems analysis tool for advanced vehicle modeling, Journal of Power Sources, 110 (2) (2002) 255-266.

[10] D. J. Friedman, T. Lipmann, A. Eggert, S. Ramaswamy, and K.-H. Hauer, Hybridization: Cost and Efficiency Comparisons for PEM Fuel Cell Vehicles, SAE, 2000-01-3078 (2000).

[11] J. M. Cunningham, M. A. Hoffman, and D. J. Friedman, A Comparison of High-Pressure and Low-Pressure Operation of PEM Fuel Cell Systems, SAE, 2001-01-0538 (2001).

[12] E. D. Doss, R. Ahluwalia, and R. Kumar, Pressurized and Atmospheric Pressure Gasoline-Fueled Polymer Electrolyte Fuel Cell System Performance, SAE, 1999-01-2574 (1999).

[13] M. Sadler, A. J. Stapleton, R. P. G. Heath, and N. S. Jackson, Application of Modeling Techniques to the Design and Development of Fuel Cell Vehicle Systems, SAE, 2001-01-0542 (2001).

[14] K. S. Jeong and B. S. Oh, Fuel economy and life-cycle cost analysis of a fuel cell hybrid vehicle, Journal of Power Sources, 105 (1) (2002) 58-65.

[15] M. M. Hussain, I. Dincer, and X. Li, A preliminary life cycle assessment of PEM fuel cell powered automobiles, Applied Thermal Engineering, 27 (13) (2007) 2294-2299.

[16] C. Liang and W. Qingnian, Energy Management Strategy and Parametric Design for Fuel Cell Family Sedan, SAE, 2003-01-1147 (2003).

[17] R. K. Ahluwalia, X. Wang, A. Rousseau, and R. Kumar, Fuel economy of hydrogen fuel cell vehicles, Journal of Power Sources, 130 (1-2) (2004) 192-201.

[18] C. N. Maxoulis, D. N. Tsinoglou, and G. C. Koltsakis, Modeling of automotive fuel cell operation in driving cycles, Energy Conversion and Management, 45 (4) (2004) 559-573.

[19] Y. Hou, M. Zhuang, and G. Wan, A transient semi-empirical voltage model of a fuel cell stack, International Journal of Hydrogen Energy, 32 (7) (2007) 857-862.

[20] M.-J. Kim and H. Peng, Power management and design optimization of fuel cell/battery hybrid vehicles, Journal of Power Sources, 165 (2) (2007) 819-832.

[21] R. K. Ahluwalia, X. Wang, and A. Rousseau, Fuel economy of hybrid fuel-cell vehicles, Journal of Power Sources, 152 (2005) 233-244.

[22] J. T. Pukrushpan, Modeling and Control of the Fuel Cell Systems and Fuel Processors, Ph. D. Thesis, University of Michigan, (2003).

[23] A. Schell, H. Peng, D. Tran, E. Stamos, C.-C. Lin, and M. J. Kim, Modelling and control strategy development for fuel cell electric vehicles, Annual Reviews in Control, 29 (1) (2005) 159-168.

[24] J. C. Amphlett, R. M. Baumert, R. F. Mann, B. A. Pepply, and P. R. Roberge, Performance modeling of the Ballard Mark IV solid polymer electrolyte fuel cell, Journal of Electrochemical Society, 142 (1) (1995) 9-15.

[25] T. E. Springer, T. A. Zawodzinski, and S. Gottesfeld, Polymer Electrolyte Fuel Cell Model, Journal of Electrochemical Society, 138 (8) (1991) 2334-2342.

[26] H.-S. Kim, D.-H. Lee, K. Min, and M. Kim, Effects of Key Operating Parameters on the Efficiency of Two Types of PEM Fuel Cell Systems (High-Pressure and Low-Pressure Operating) for Automotive Applications, Journal of Mechanical Science and Techonolgy, 19 (4) (2005) 1018-1026.

[27] D.-H. Lee, Performance Analysis of PEM Fuel Cell System Including BOP According to the Change of Air Supply System, Master Thesis, Seoul National University, (2005).

[28] R. M. Moore, K. H. Hauer, S. Ramaswamy, and J. M. Cunningham, Energy utilization and efficiency analysis for hydrogen fuel cell vehicles, Journal of Power Sources, 159 (2) (2006) 1214-1230.

[29] J.-H. Wee, Applications of proton exchange membrane fuel cell systems, Renewable and Sustainable Energy Reviews, 11 (8) (2007) 1720-1738.

[30] M. B. V. Virji and R. H. Thring, Analysis of a 50 kWe indirect methanol proton exchange membrane fuel cell (PEMFC) system for transportation application, Journal of Automobile Engineering, Part D, 219 (2005) 937-950.

[31] Y. Hou, M. Zhuang, and G. Wan, The analysis for the efficiency properties of the fuel cell engine, Renewable Energy, 32 (7) (2007) 1175-1186.